Research Article

Journal of Environmental Nanotechnology

Seed Extract-mediated Cu-Doped TiO_2 Nanoparticles: Linking Morphological Evolution with Optical and Antibacterial Properties

Deepthy P Nair and E. Sivasenthil*
Department of Physics, Karpagam Academy of Higher Education, Eachanari, Coimbatore, TN, India
Received: 29.06.2026 Accepted: 28.07.2026 Published: xx.xx.xxxx
*sivasenthil.e@kahedu.edu.in

ABSTRACT

Green synthesis of semiconductor nanomaterials offers a sustainable approach for developing functional materials with enhanced physicochemical properties. In this study, Cu-doped(1wt%) TiO_2 nanoparticles were synthesized through a modified sol-gel method using extracts of five different plant seeds, namely *Papaya*, *Bitter gourd*, *Gokshura*, *Drumstick* and *Tamarind* as natural reducing and capping agents. Each of these garden seeds, found in plenty in Indian households, is rich in different types of phytochemicals. The study here shows the implicit relation between the influence of various phytochemicals on the structural and functional properties of biosynthesized nanoparticles. This comparison shows how each bio compound differently influences the synthesis process, which lies at the novelty of the study. The influence of seed-derived phytochemicals on the morphological, optical and antibacterial properties of the nanoparticles was systematically investigated. X-ray diffraction confirmed the formation of phase-pure anatase TiO_2 with crystallite sizes ranging from 8.1 to 10.4 nm. This indicates the different capping capacity of different plant extracts, while SEM revealed extract-dependent variations in particle morphology and porosity. EDX analysis verified Cu presence, and FTIR confirmed the presence of residual phytochemicals acting as surface stabilizers. Diffuse reflectance spectroscopy demonstrated indirect optical band-gap energies between 2.63 and 3.09 eV, indicating enhanced visible-light absorption compared with pristine TiO_2, keeping similar doping conditions. The PL spectra exhibited a marked decrease in emission intensity, indicating suppressed electron–hole recombination. The combined observations suggest that Cu doping and phytochemical-assisted green synthesis may have introduced defect or intermediate energy states that facilitate charge separation while simultaneously extending visible-light absorption. The Sd sample exhibited the lowest band gap (2.63 eV), suggesting superior bandgap tuning, whereas the St sample showed the highest band gap (3.09 eV). All synthesized nanoparticles exhibited antibacterial activity against *Escherichia coli* and *Staphylococcus aureus*, with Sp showing the highest inhibition against *E. coli* (12.7 ± 0.14 mm) and Sg against *S. aureus* (11.0 ± 0.28 mm). The study demonstrates that seed phytochemistry provides an effective route for fabricating Cu-doped TiO_2 nanomaterials with controlled crystallite size and reduced band gap, which thereby foster their antibacterial activity against Gram-negative and Gram- positive bacteria.

Keywords: Antibacterial activity; Phytochemicals; *Papaya*; *Bitter gourd*; *Gokshura*; Drum-stick and *Tamarind*.

1. INTRODUCTION

Titanium dioxide (TiO_2) is one of the most widely investigated semiconductor metal oxides due to its excellent chemical stability, non-toxicity, low cost and higher photocatalytic and antimicrobial properties. These characteristics have led to its wide application in environmental modifications (Ganesan *et al.* 2024), energy conversion (Parangi and Mishra, *et al.* 2021), self-cleaning coatings (Srivastava *et al.* 2025), sensors (Nunes *et al.* 2022) and biomedical fields. However, the practical performance of pure TiO_2 is often limited by its wide band gap and rapid recombination of photogenerated charge carriers. This restricts its efficiency under visible light irradiation. To overcome these limitations, different modification strategies like metal ion doping, non-metal doping and surface functionalization have been implemented. Among the various dopants, copper (Cu) has attracted attention due to its ability to alter the electronic structure of TiO_2, improve visible light absorption, reduce electron–hole recombination and make a better photocatalytic performance. Cu-doped TiO_2 nanomaterials have demonstrated superior optical (Tien *et al.* 2026), catalytic (Mingmongkol *et al.* 2022) and antimicrobial (Wojcieszak *et al.* 2017) properties compared to pristine TiO_2, making them promising candidates for environmental and biomedical applications.

In recent years, increasing concerns regarding environmental sustainability and the dangerous effects associated with chemical synthesis methods have encouraged the development of green synthesis approaches for nanomaterial fabrication. Green synthesis utilizes naturally occurring phytochemicals present in plant extracts as reducing, stabilizing, and capping agents, thereby minimizing the use of toxic chemicals and reducing environmental impact (Singhal *et al.* 2022). Plant-mediated synthesis is particularly attractive because it is simple, cost-effective, eco-friendly, and scalable (Oliveira and Lenzi, 2023).

Seed extracts constitute a rich source of bioactive compounds, including polyphenols, flavonoids, alkaloids, proteins, carbohydrates, and other secondary metabolites (Sławińska and Olas, 2022; Coyago-Cruz *et al.* 2025). These phytochemicals can significantly influence nucleation, crystal growth, particle stabilization, and surface modification during nanoparticle synthesis (Bodor *et al.* 2025). Hence, the nature and composition of the seed extract used may affect the structural, morphological, optical and biological properties of the synthesized nanomaterials (Bhardwaj *et al.* 2022). Although numerous studies have reported the green synthesis of Cu-doped TiO_2 nanoparticles using individual plant extracts, systematic comparisons of different botanical sources remain scarce. In particular, comparative investigations involving multiple seed extracts under identical synthesis conditions, together with their influence on the structural, optical, and photovoltaic performance of Cu-doped TiO_2 photoanodes, have not been adequately explored. Addressing this gap, the present study synthesizes Cu-doped TiO_2 nanoparticles using five individual seed extracts via a green synthesis approach. Understanding the role of various phytochemical environments in tailoring material characteristics is essential for optimizing synthesis protocols and enhancing functional performance.

Therefore, the present study focuses on the green synthesis of Cu-doped TiO_2 nanoparticles using five different seed extracts as biogenic mediators. The seeds, phytochemical composition of which is much known through former studies used here are *Papaya* seeds (Rani *et al.* 2023), *Bittergaurd seeds* (Oyelere *et al.* 2022), *Gokshura* seeds (Chhatre *et al.* 2014),*Drumstick* seeds (Saini *et al.* 2016) and *Tamarind* seeds (Ganesapillai *et al.* 2017) identidied by sample names *Sp, Sb, Sg, Sd and St* respectively abbrevating the first letter of each seed name. The selected seeds exhibit distinct phytochemical profiles, enabling investigation of how variations in naturally occurring reducing and stabilizing biomolecules affect the nucleation, growth, crystallinity, optical behaviour and antibacterial activity of Cu-doped TiO_2 nanoparticles. The chosen seeds are inexpensive, readily available agricultural materials or by-products in South India. These seeds are widely reported in traditional medicine for their antioxidant and antimicrobial activities, suggesting the presence of bioactive metabolites capable of acting as reducing, chelating, and capping agents during nanoparticle synthesis (Singh *et al.* 2013; Bonin *et al.* 2023; Abbas *et al.* 2024; AlSedairy *et al.* 2025). The synthesized materials were characterized to evaluate their morphological and optical properties and to investigate the influence of the selected seed extracts on nanoparticle formation. Also, their antibacterial activity was assessed against pathogenic bacterial strains to establish correlations between synthesis conditions, physicochemical characteristics and biological performance. The type and concentration of capping or stabilizing agents influence the size, morphology, and surface characteristics of nanoparticles, which may consequently affect their functional properties, including antibacterial activity. However, the contribution of morphology to antibacterial performance is often accompanied by other physicochemical factors such as particle size, surface chemistry and composition This comparative study provides insights into the role of seed-derived phytochemicals in governing the properties of Cu-doped TiO_2 nanomaterials and specifies the potential of sustainable plant-mediated synthesis routes for advanced antimicrobial applications.

2. MATERIALS AND METHODS

2.1 Materials

Titanium Isopropoxide 27.8-28.6 TTIP), Copper Nitrate Trihydrate, Glacial Acetic acid (All purchased from Sisco Research Laboratories India) and the extracts of the five different seeds mentioned above. All the chemicals were purchased from Sisco Research Laboratories India directly.

2.2 Synthesis of Cu Doped TiO_2 Nanocomposite

The doped TiO_2 Nanoparticles(1wt%) with copper were synthesized by the modified sol-gel method. Copper concentration of 1wt% was selected based on previous studies demonstrating that low Cu loading effectively modifies the electronic structure and optical properties of TiO_2 while maintaining the anatase crystal structure (Ganesh *et al.* 2014). Here, the copper dopant was stabilized with the green extract before beginning the doping process.

2.2.1 Preparation of Green Extract

Seeds of all the above-given five plants were collected from the garden, washed and sun-dried to prepare individual powders. Dried seeds were taken and crushed to powder them. 10 gm of each powder was added to a glass jar and mixed with ethanol and distilled water in the ratio 4:1(80 mL ethanol and 20 mL distilled water) and was covered. The jar was placed undisturbed for a week at room temperature with occasional stirring. The seed powders were extracted by maceration in ethanol for 7 days at room temperature following established phytochemical extraction protocols (Kaur *et al.* 2022). After a week, the extract was filtered using Whitemans filter paper and preserved in amber glass bottles in refrigeration. About 90ml of extract was obtained. Since the extract was employed in its liquid form without solvent evaporation, the percentage extraction yield and extract concentration were not quantitatively determined. To ensure consistency among all botanical extracts, identical extraction conditions, including plant mass, solvent composition, solvent volume, extraction duration, and filtration procedure, were maintained for all samples

2.2.2 Synthesis of TiO_2-Cu Nanoparticles

The modified Sol Gel method here employs the mixing of copper dopant with green extract to prepare the precursor. Copper nitrate trihydrate at 1wt% (0.766mM of Cu) was dissolved in 10ml of green extract and stirred for 10 minutes.10ml of Titanium isopropoxide was slowly added to 100 mL of isopropanol with mild heating and stirring. Glacial acetic acid(1ml) was added to this. The copper precursor was slowly added with rapid stirring at 80^0 C for about one and a half hours. The solution thickened. Colours ranged from green to light brown. The final gel-like material was dried overnight in an oven at 80^O C for 8 hours. The dried sample was then calcined at 350^OC for 3 hours. In earlier studies, it was confirmed that calcination at 350°C produced pure anatase TiO_2, whereas higher temperatures (500–700°C) resulted in mixed anatase–rutile phases and 800°C produced rutile (Rajaram *et al.* 2023)

2.3 Material Characterization of Cu Infused TiO_2 Nanocomposite

Structural morphology was analysed using Scanning electron microscopy(SEM)

using the OXFORD XMX N (STIC India, Kochi). Surface morphology was examined using a scanning electron microscope operated at an accelerating voltage of 20 kV. The surface texture of nanoparticles is assessed. The chemical composition is checked, and successful doping is confirmed using an Energy Dispersive X-ray spectrometer (EDAX) study. Bruker D8 Advance is used to examine the crystallite size by powder X-ray diffraction. X-ray diffraction (XRD) patterns were recorded with Cu Kα radiation ($\lambda = 1.5406$ Å) over a 2θ range of 10–80° at a step size of 0.02°. The organic functional groups are checked by Fourier Transform infrared spectroscopy (FTIR). FTIR spectra were recorded in the range of 4000–400 cm^{-1}. Band gap variations are studied through Diffuse Reflectance Spectroscopy (DRS). Diffuse reflectance spectra were recorded over the wavelength range of 200–800 nm. All of the Characterization tests were performed at the Sophisticated Test and Instrumentation Centre(STIC India), Kochi, Kerala.

2.3.1 Antibacterial Properties of Nanocomposite

The synthesized nanocomposite is tested for its antimicrobial properties against Gram-positive and Gram-negative bacteria. Considering the diverse applications of Cu-doped TiO_2 nanomaterials, antibacterial activity has attracted considerable attention owing to the increasing prevalence of multidrug-resistant pathogenic microorganisms. Incorporation of Cu into the TiO_2 lattice promotes oxygen-vacancy formation, improves charge separation and enhances reactive oxygen species (ROS) generation, which contribute to bacterial membrane disruption, protein oxidation and DNA damage. Moreover, Cu^{2+} ions themselves exhibit intrinsic antimicrobial activity through interactions with bacterial cell membranes and intracellular biomolecules. Green synthesis further introduces phytochemical-derived surface functionalities that improve nanoparticle dispersion and surface interactions with microbial cells. Therefore, antibacterial evaluation represents an appropriate model application for correlating the structural and optical modifications induced by phytochemical-assisted Cu doping with the functional performance of the synthesized nanoparticles. In the present case, the antimicrobials present in the given sample were allowed to diffuse out into the medium and interact in a plate freshly seeded with the test organisms. The resulting zones of inhibition were uniformly circular as there was a confluent lawn of growth (Bauer *et al.* 1959a). The diameter of the zone of inhibition was measured in millimeters. All experiments were performed in triplicate (n = 3), and the results are presented as mean ± standard deviation (SD). The simple T-test was performed using GraphPad Prism software 8.0, and the SD was calculated using MS Excel. The required bacteria (*E. coli* – 443 and *S. aureus* – 902) were purchased from MTCC Chandigarh, India. Nutrient Agar medium, Nutrient broth, and Gentamicin discs were purchased from Himedia, India. Test samples, Petri plates, test tubes, beakers, and conical flasks were from Borosil, India.

3. RESULTS AND DISCUSSIONS

3.1 Scanning Electron Microscopy (SEM) Analysis

The SEM image of the synthesized Cu- TiO_2 nanocomposite using extracts of the five different seeds is given below (Figure 1). Sample Sb shows a smooth surface with dispersed nano-clusters and clear edges with moderate agglomeration. Sd gives broken flakes with mixed irregular blocks. More interparticle voids than Sb are present. Sg has a mixed grain size distribution. However, Sp shows dense-packed irregular grains and moderate roughness. St gives overgrown grains. So, together we can say SEM micrographs of seed-mediated Cu-doped TiO_2 nanoparticles revealed agglomerated micro-grains composed of finer nanostructures. SEM analysis revealed differences in particle morphology and the degree of agglomeration among the synthesized Cu-doped TiO_2 samples. Samples exhibiting relatively smaller and more uniformly distributed nanoparticles may provide a more accessible surface area for interaction with incident light and bacterial cells. However, SEM observations alone cannot establish the origin of the improved functional performance.

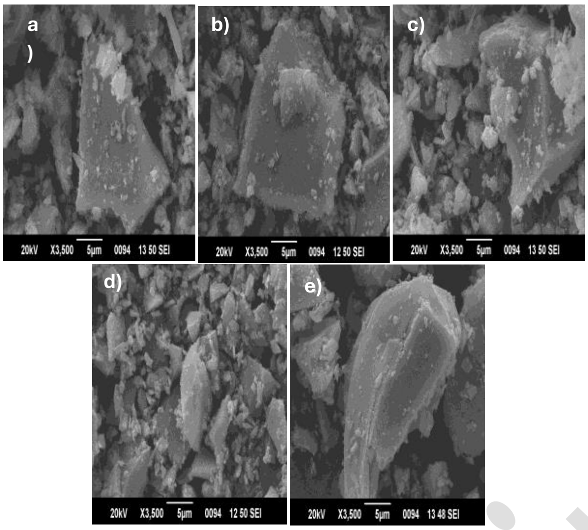

Fig. 1: SEM images of samples (a)Sb (b)Sd (c)Sg (d)Sp and (e)St

3.2 Energy Dispersive X-Ray Spectroscopy (EDX) Analysis

The surface analysis of the samples is done using EDX Spectroscopy. Figure 2 shows the graphical representation of the spectral analysis. In all five samples, we can observe clear Ti and O peaks along with Cu peaks. The Cu peak intensity here depends upon the variation in surface incorporation of Cu in the synthesized samples. Sb achieved the highest Cu loading (1.77wt%), meaning that seed extract likely had stronger reducing/chelating phytochemicals for Cu attachment. St had the lowest identified Cu presence. Similarly, Sb may contain more oxygen vacancies. Summarizing, EDAX analysis confirmed Ti, O, and Cu in all seed-mediated Cu-doped TiO_2 nanoparticles with relatively uniform elemental incorporation of copper within the analysed regions. (Ahmadiasl *et al.* 2022). Copper content varied from 0.55 to 1.77 wt%, indicating that seed phytochemicals may have affected Cu doping efficiency. However, EDX does not provide direct evidence of substitutional lattice incorporation or the oxidation state of Cu. Therefore, definitive confirmation of lattice doping would require complementary techniques such as XPS or EPR.

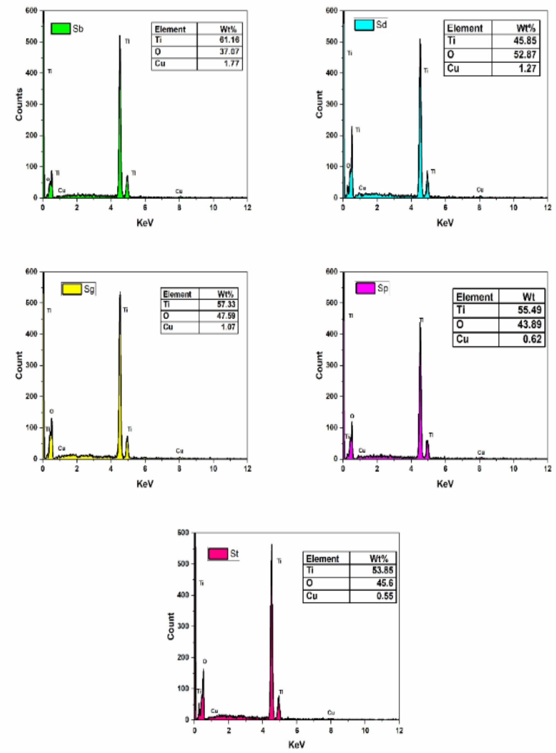

Fig. 2: EDX spectra of samples Sb, Sd, Sg, Sp and St

3.3 X-Ray Diffraction (XRD) Analysis

Analysing the X-ray diffraction data obtained from the samples, a graphical representation of the relation between the diffracting angle and intensity is plotted. Samples exhibit diffraction peaks at approximately 25.3°, 37.8°, 48.0°, 54.0°, 62.7°, 68.8°, and 75.0°, corresponding to the crystallographic planes (101), (004), (200), (105), (204), (116), and (215), respectively. These peaks match well with the standard anatase TiO_2 phase (JCPDS card No. 89-4921), confirming the successful formation of anatase-structured TiO_2 in all samples (Perarasan *et al.* 2019) The characteristic anatase peak ($2\theta \approx 25.3°$) corresponding to the (101) plane is the most intense reflection in all samples, indicating that anatase is the dominant crystalline phase. No additional peaks associated with rutile TiO_2, brookite TiO_2, CuO, Cu_2O or metallic Cu are observed within the detection limit of the instrument. This suggests that Copper ions are either incorporated into the TiO_2 lattice through substitutional doping or that the Cu concentration remains below the XRD detection limit. The graphical representation is given below in Figure 3.

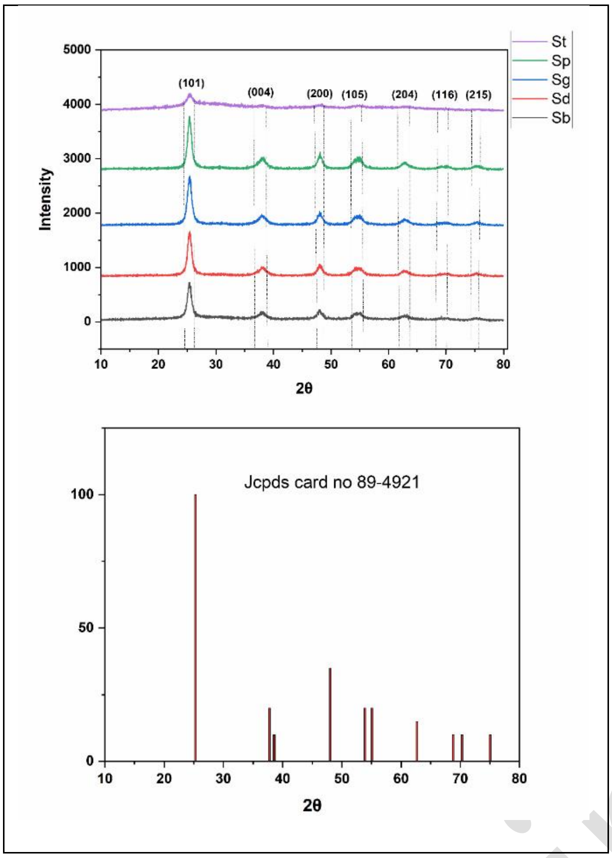

Fig. 3: XRD patterns of samples St, Sp, Sg, Sd and Sb

The crystallite size was estimated using the Debye–Scherrer equation given by

$$D = \frac{K\lambda}{\beta \cos \Theta} \quad \dots (1)$$

where K=0.89, λ=1.5406 Å (Cu Kα radiation), β is the full width at half maximum (FWHM) corrected for the instrumental broadening reported by the Bruker DIFFRAC.EVA software, and θ is the Bragg diffraction angle. The software automatically performs $K\alpha_2$ stripping, determines the FWHM of the selected diffraction peaks, applies the specified instrumental broadening (0.050°) and calculates the crystallite size according to the Debye–Scherrer equation. The same analysis protocol was applied to all synthesized samples.An average of the three calculated size is considered to be the average crystallite size. Representative FWHM values corresponding to the principal diffraction peaks used for the Scherrer equation calculations for one sample (Sb) is included below in Table 1.

Table 1. Crystallite size calculation using FWHM for sample Sb

Peak (2θ)	Plane (hkl)	FWHM (°)	Crystallite Size (nm)
25.43	(101)	0.779	10.4
38.03	(004)	1.053	7.9
48.04	(200)	0.774	11.1

Similar calculations are done for each sample using the DIFFRAC.EVA software. The crystallite sizes of green-synthesized Cu-doped TiO_2 nanoparticles varied from 8.6 to 9.8 nm depending on the seed extract used. Sb exhibited the highest average crystallite size, whereas St showed the smallest size, indicating that phytochemicals present in the seed extracts significantly influenced nucleation and crystal growth. The crystallite size for each sample is given below in Table 2

Table 2. Average crystallite size for each nanocomposite sample

Label	Calculated Sizes (nm)	Average Size (nm)
Sb	10.4, 7.9, 11.1	9.8
Sd	9.8, 6, 10	8.6
Sg	9.2, 6.1, 10.3	8.5
Sp	10.2,6.4, 11.3	9.3
St	6.4, 9.7	8.1

3.4 Fourier Transform Infrared Spectroscopy (FTIR) Analysis

The FTIR spectra of the Cu-doped TiO_2 nanoparticles synthesized using five different seed extracts exhibit several characteristic absorption bands corresponding to Ti–O bonding and residual phytochemical groups derived from the green material. The differences in band intensity among the samples indicate that the seed precursor influenced the surface chemistry and capping of the nanoparticles. The absorption band in the 400–700 cm^{-1} region is primarily attributed to Ti–O–Ti lattice vibrations. Bands in the 850–1500 cm^{-1} show several peaks. Region around 950–1050 cm^{-1} identifies C–O–C groups from polyphenols and carbohydrates which may have been present in seed extracts. Around 1100–1250 cm^{-1}, peaks depict either alcoholic C–O stretching or polysaccharides s plant metabolites. Peaks around 1300–1450 cm^{-1} correspond to C–H bending vibrations. These peaks indicate that phytochemicals from the seed extracts remain adsorbed on the nanoparticle surface and act as stabilizing/capping agents. Weak bands near 1550–1650 cm^{-1} may arise from C=O stretching of carbonyl compounds. A broad region around 3200–3600 cm^{-1} is weakly visible in some samples, which stands for surface hydroxyl groups or adsorbed moisture (Maragatha et al. 2016). Sp and Sg Samples give the strongest organic functional group absorption. Sd gives good nanoparticle formation with lower residual organics. St has the lowest organic content. Minor changes in band position or intensity following Cu addition may indicate alterations in the local bonding environment. However, FTIR spectroscopy alone cannot conclusively identify Ti–O–Cu bond formation, and therefore these spectral changes are interpreted as evidence of structural modification rather than direct confirmation of specific chemical bonding. The transmittance percentage versus wavenumber graph is given below in Figure 4.

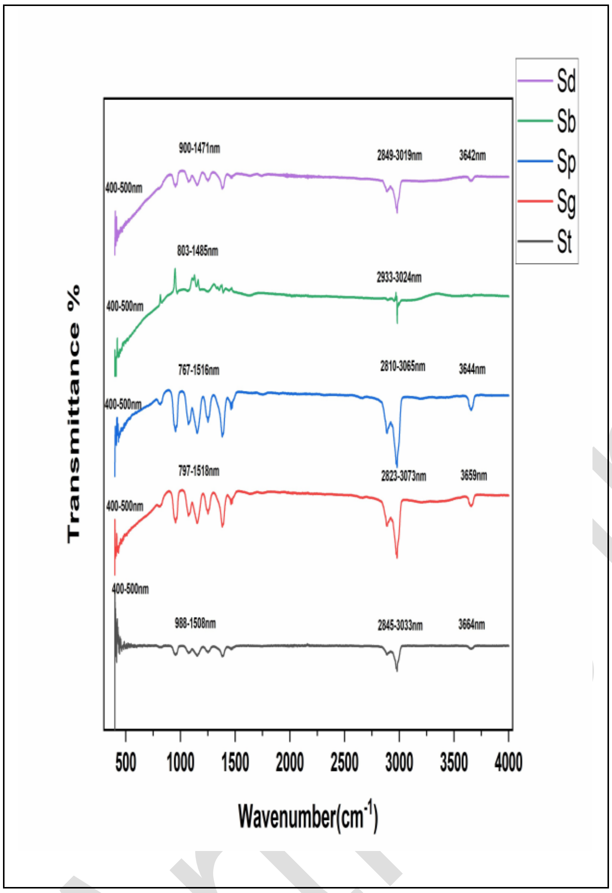

Fig. 4: FTIR spectra of five seed samples

3.5 Diffuse Reflectance Spectroscopy(UV-Vis) Analysis

The indirect optical band-gap energies of the Cu-doped TiO_2 nanoparticles synthesized using different seed samples ranged from 2.63 to 3.09 eV. This indicates successful band-gap narrowing relative to pristine anatase TiO_2. Among the samples, Sd exhibited the lowest band gap (2.63 eV). The reduced optical band gap observed for the Cu-containing TiO_2 nanoparticles indicates a modification of the electronic structure. However, the present characterization techniques do not permit direct identification of oxygen vacancies or defect states, and therefore no definitive attribution is made. In contrast, the St sample synthesized using *Tamarind* seed extract showed the highest band gap (3.09 eV). This behaviour may be caused by the unique phytochemical composition of *Tamarind* seeds, which are rich in tannins and polysaccharides. These strongly chelate Cu^{2+} ions during the sol-gel process, reducing Cu doping into the TiO_2 lattice. The absence of secondary crystalline phases in XRD confirms that the optical variations arise primarily from differences in defect chemistry and surface characteristics rather than phase transformation. From the obtained transmittance data, a Tauc curve is plotted for each sample as given in Figure 5 below

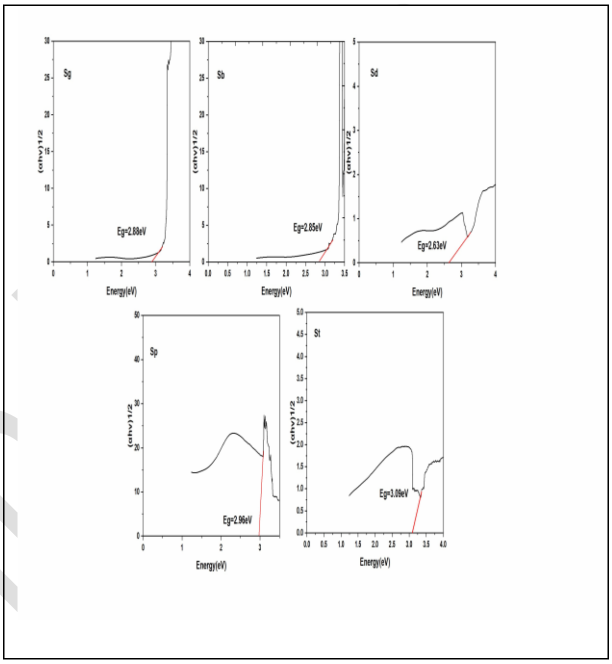

Fig. 5: Tauc curve for samples Sp, Sg, Sb, Sd and St

The plot clearly shows a reduction in Eg in all the given samples. Doping with copper, which is a transitional metal, may develop intermediate energy levels, resulting in a more narrow band gap. Between all the samples, Sd is expected to possess the highest photocatalytic efficiency and is likely to exhibit superior pollutant degradation and antibacterial performance due to improved charge separation (Yoshida, 2024). The two samples, Sg and Sb, have very similar band gaps. Materials with similar band gaps were previously used for DSSC applications and in self-cleaning coatings according to earlier literature (Alcazar *et al.* 2026).

3.6 Antibacterial Activity

The antibacterial activity of Cu-doped TiO_2 nanoparticles synthesized using different seed samples was evaluated against *E. coli* and *S. aureus* using the disc diffusion method as shown in Figure 6. Petri plates containing 20 mL nutrient agar medium were seeded with a 24-hour culture of bacterial strains that were adjusted to a 0.5 OD value according to the McFarland standard. The discs containing the test samples Sg, Sp, St, Sb and

Sd were placed on the respective agar plates. The plates were then incubated at 37°C for 24 hours. The antibacterial activity was assayed by measuring the diameter of the inhibition zone formed around the discs. Gentamicin discs were used as a positive control. (Bauer *et al.* 1959a) All synthesized samples exhibited measurable antibacterial activity, although the extent of inhibition varied depending on the seed extract employed during synthesis. Against *E. coli*, the Sp sample demonstrated the highest antibacterial activity with a zone of inhibition of 12.7 ± 0.14 mm, followed by Sd, Sb, Sg, and St. In contrast, Sg exhibited the strongest activity against *S. aureus* with a zone of inhibition of 11.0 ± 0.28 mm, followed by Sp and Sd. The observed differences suggest that the phytochemical composition of the seed-derived solvent significantly influences nanoparticle surface properties and antibacterial efficacy. The enhanced antibacterial activity of the Sp and Sg samples may be due to their superior crystallinity, introduction of Cu and the presence of surface-bound bioactive phytochemicals. The observed antibacterial activity given in Figure 7 may be associated with mechanisms reported for metal oxide nanoparticles, including oxidative stress and interactions with the bacterial cell envelope. However, these mechanisms were not experimentally investigated in the present study, and therefore no definitive mechanistic conclusions are drawn. The lower activity observed for St indicates comparatively weaker nanoparticle-bacteria interactions. Overall, the results demonstrate that green synthesis using different seed extracts can effectively tailor the antibacterial performance of Cu-doped TiO_2 nanoparticles, highlighting their potential for biomedical and antimicrobial applications.

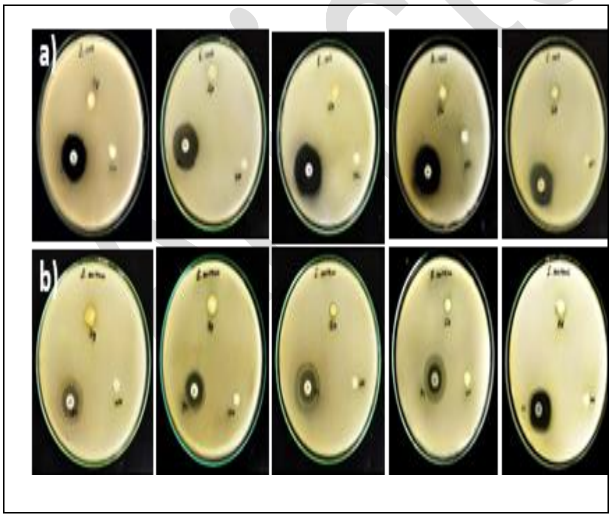

Fig. 6: Antibacterial assay of five samples against bacteria (a) *E. Coli* and (b) *S. Aureus*

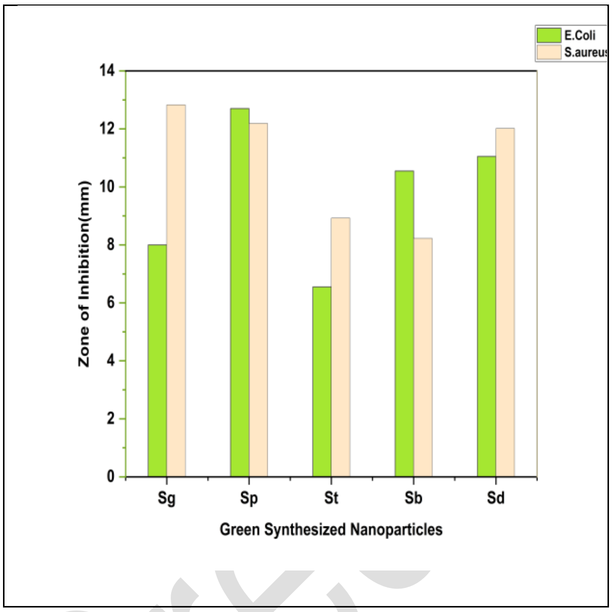

Fig. 7: Comparison of antibacterial activity of 5 samples against *E. Coli* and *S. aureus*

4. CONCLUSION

In the present study, Cu-doped TiO_2 nanoparticles were successfully synthesized through a sustainable green sol-gel approach using five different seed extracts as biogenic mediators. The study shows that the phytochemical composition of the seed extracts may play an important role in controlling the structural, morphological, optical and antibacterial properties of the synthesized nanoparticles. XRD analysis confirmed the formation of phase-pure anatase TiO_2 in all samples without detectable secondary copper oxide phases. Considering the low Cu concentration together with the absence of detectable crystalline Cu oxide phases, Cu is likely to exist as highly dispersed species or to be partially incorporated into the TiO_2 framework. Nevertheless, definitive confirmation of lattice substitution would require techniques such as XPS, Raman spectroscopy, EXAFS or XANES. The crystallite sizes confirm the formation of nanoscale materials with extract-dependent crystal growth behaviour.

EDX analysis verified the presence of Ti, O and Cu in all samples and revealed variations in Cu presence on the region examined. This may be due to the presence of different phytochemical environments during synthesis. FTIR spectra further confirmed the presence of residual surface phytochemicals that acted as natural capping and stabilizing agents.

Diffuse reflectance spectroscopy demonstrated successful band-gap engineering, with varying indirect optical band-gap energies indicating enhanced visible-light absorption compared to pristine TiO_2. Materials with similar band gaps were previously used for DSSC applications and in self-cleaning coatings according to earlier literature (Alcazar *et al.* 2026) and hence can be considered as prospects for future investigations. The antibacterial studies confirmed that all synthesized nanoparticles possessed activity against both Gram-positive and Gram-negative bacteria, although their effectiveness varied depending on the seed extract utilized. The synthesized Cu-doped TiO_2 nanoparticles exhibited distinct structural, morphological, optical and antibacterial characteristics. While variations among these properties were observed, the present study did not establish direct causal relationships between morphology, optical properties, and antibacterial performance. The enhanced optical response and antibacterial activity are interpreted in conjunction with the reduced optical band gap, suppressed PL emission intensity and the experimental antibacterial results, suggesting that both morphological and electronic modifications collectively contribute to the observed performance.

Overall, this study establishes that seed-mediated green synthesis is an effective strategy for the physio-chemical and biological properties of Cu-doped TiO_2 nanoparticles. The results demonstrate that careful selection of plant-derived phytochemicals enables controlled modification of nanoparticle properties, thereby allowing the design of nanomaterials for specific applications. The synthesized Cu-doped TiO_2 nanoparticles show considerable promise for antibacterial applications. This study presents a systematic comparative investigation of five different botanical seed extracts for the green synthesis of Cu-containing TiO_2 nanoparticles under identical experimental conditions. The results demonstrate that the choice of seed extract influences the structural, morphological, optical and antibacterial characteristics of the synthesized nanoparticles. Rather than proposing mechanistic explanations beyond the available evidence, this work provides an experimental comparison of botanical extract-assisted synthesis and establishes a foundation for future studies employing advanced spectroscopic characterization and mechanistic investigations. Future studies may analyse the applicability of the samples for photocatalysis and self-cleaning surfaces, environmental remediation and other sustainable nanotechnology applications.

ACKNOWLEDGMENTS

Sincere gratitude to my Guide and Mentor, Dr. E. Siva Senthil, for his timely assistance and guidance. Sincere gratitude to the Head of the Department, Dr. Janardanan, and the entire Department of Physics, Karpagam Academy of Higher Education, for continuous support and encouragement. Sincere gratitude to DST SAIF Cochin for all the support in material testing and analysis.

STATEMENTS AND DECLARATIONS

There are no financial or non-financial interests that are directly or indirectly related to the work submitted hereby for publication.

FUNDING

This research received no specific grant from any funding agency in the public, commercial, or not-for-profit sectors.

CONFLICTS OF INTEREST

The authors declare that there is no conflict of interest.

REFERENCES

Abbas, M., Shabbir, M. A., Haq, S. M. A. U., Wahab, H. A., Hassan, S. A., Adeeba, F., Ali, A., Asif, M., Nasir, A., Khaneghah, A. M. and Aadil, R. M., Harnessing the potential of *Bitter gourd* seeds for food and nutrition- A comprehensive review, *Appl. Food Res.*, 4(2), 100508(2024). https://doi.org/10.1016/j.afres.2024.100508

Ahmadiasl, R., Moussavi, G., Shekoohiyan, S. and Razavian, F., Synthesis of Cu-Doped TiO_2 Nanocatalyst for the Enhanced Photocatalytic Degradation and Mineralization of Gabapentin under UVA/LED Irradiation: Characterization and Photocatalytic Activity, *Catal.*, 12(11), 1310 (2022). https://doi.org/10.3390/catal12111310

Alcazar, K., Tous, L., Herrera, A., Martinez-Bernett, D. and Saba, M., TIO_2 nanoparticles obtained by green synthesis: Characterization and evaluation of their effect on the Self-Cleaning and antifungal properties of an aqueous Paint-Type coating, *Nanomater.*, 16(2), 91 (2026). https://doi.org/10.3390/nano16020091

AlSedairy, S. A., Aziz, I. M., Alshalan, R. M., Farrag, M. A., Almuqrin, A. M., Alghamdi, A. K. and Aljowaie, R. M., Bioactive Compounds, Antibacterial, Antioxidant, Anticancer, and Antidiabetic Potential of the Seed and Leaves of Tribulus terrestris, *Life*, 15(12), 1799 (2025). https://doi.org/10.3390/life15121799

Bauer, A. W. M. D., David, M. P., William, M. M. and Kibby, M. D., Single-disk antibiotic-sensitivity testing of staphylococci: An analysis of technique and results, *JAMA Int. Med.*, 104(2), 208-216(1959a). https://doi.org/10.1001/archinte.1959.00270080034004

Bauer, A. W., Robertson, C. E. and Kirby, W. M., Single disc versus multiple disc and plate dilution techniques for antibiotic sensitivity testing, *Antibio. Annual,* 7, 574-580(1959b).

Bhardwaj, K., Chopra, C., Bhardwaj, P., Dhanjal, D. S., Singh, R., Najda, A., Cruz-Martins, N., Singh, S., Sharma, R., Kuča, K. and Manickam, S., Biogenic Metallic Nanoparticles from Seed Extracts: Characteristics, Properties, and Applications, *J. Nanomater.*, 2022(1), 2271278(2022). https://doi.org/10.1155/2022/2271278

Bodor, T., Fejes, G., Kondak, D., Kondak, S., Szőllősi, R., Da Silva, R. C., Rónavári, A., Kónya, Z. and Kolbert, Z., Seeds and nanomaterials: seed-assisted synthesis, nanotoxicity, and seed-associated nanotechnology innovations, *J. Exp. Bot.*, 77(7), 1991–2012(2025). https://doi.org/10.1093/jxb/eraf402

Bonin, E., Avila, V. D., Carvalho, V. M., Cardoso, M. a. P., Matos, A. M., Ramos, A. V. G., Cabral, M. R. P., Baldoqui, D. C., Sarragiotto, M. H., De Abreu Filho, B. A. and Prado, I. N. D., Study of chemical constituents, antioxidants and antimicrobial activities of *Tamarind*us indica L. seed, *J. Food Sci*., 88(11), 4639–4652(2023). https://doi.org/10.1111/1750-3841.16739

Chhatre, S., Nesari, T., Kanchan, D., Somani, G. and Sathaye, S., Phytopharmacological overview of Tribulus terrestris, *Pharmacognosy Rev.*, 8(15), 45(2014). https://doi.org/10.4103/0973-7847.125530

Coyago-Cruz, E., Salazar, I., Guachamin, A., Alomoto, M., Cerna, M., Mendez, G., Heredia-Moya, J. and Vera, E., Bioactive compounds, antioxidant, and antimicrobial activity of seeds and mucilage of non-traditional cocoas, *Antiox*., 14(3), 299(2025). https://doi.org/10.3390/antiox14030299

Ganesan, S., Roshan, P. and Mathur, R., Photocatalyst Based on TIO_2 and its Application for environmental Remediation: A Challenge to Sustainable development, *Bentham Sci. Publish*., 2, 253–272 (2024). https://doi.org/10.2174/9789815165586124020025

Ganesapillai, M., Venugopal, A. and Simha, P., Preliminary isolation, recovery and characterization of polyphenols from waste *Tamarind*us indica L, *Mater. Today Proce*., 4(9), 10658-10661 (2017). https://doi.org/10.1016/j.matpr.2017.06.438

Ganesh, I., Kumar, P. P., Annapoorna, I., Sumliner, J. M., Ramakrishna, M., Hebalkar, N. Y., Padmanabham, G. and Sundararajan, G., Preparation and characterization of Cu-doped TiO_2 materials for electrochemical, photoelectrochemical, and photocatalytic applications, *Appl. Surf. Sci*., 293, 229–247(2014). https://doi.org/10.1016/j.apsusc.2013.12.140

Kaur, A., Sharma, Y., Kumar, A., Ghosh, M. P. and Bala, K., In-vitro antiproliferative efficacy of Abrus precatorius seed extracts on cervical carcinoma, *Sci. Rep.*, 12(1), 10226. (2022). https://doi.org/10.1038/s41598-022-13976-7

Maragatha, J., Rajendran, S., Endo, T. and Karuppuchamy, S., Microwave synthesis of metal doped TiO_2 for photocatalytic applications, *J. Mater. Sci. Mater. Electron.*, 28(7), 5281–5287(2016). https://doi.org/10.1007/s10854-016-6185-7

Mingmongkol, Y., Trinh, D. T. T., Phuinthiang, P., Channei, D., Ratananikom, K., Nakaruk, A. and Khanitchaidecha, W., Enhanced photocatalytic and photokilling activities of CU-Doped TIO_2 nanoparticles, *Nanomater.*, 12(7), 1198(2022). https://doi.org/10.3390/nano12071198

Nunes, D., Fortunato, E. and Martins, R., Flexible nanostructured TiO_2-based gas and UV sensors: a review, *Discover Mater.*, 2(1), 2(2022). https://doi.org/10.1007/s43939-022-00023-5

Oliveira, J. R. and Lenzi, G. G., Advances in the use of green and sustainable synthesis to obtain nanomaterials, *IntechOpen*, (2023). https://doi.org/10.5772/intechopen.1002866

Oyelere, S. F., Ajayi, O. H., Ayoade, T. E., Pereira, G. B. S., Owoyemi, B. C. D., Ilesanmi, A. O. and Akinyemi, O. A., A detailed review on the phytochemical profiles and anti-diabetic mechanisms of Momordica charantia, *Heliyon*, 8(4), e09253(2022). https://doi.org/10.1016/j.heliyon.2022.e09253

Parangi, T. and Mishra, M., Titanium Dioxide as Energy Storage Material: A Review on Recent Advancement, *IntechOpen*, (2021). https://doi.org/10.5772/INTECHOPEN.99254

Perarasan, T., Peter, I. J., Kumar, A. M., Rajamanickam, N., Ramachandran, K. and Mohan, C. R., Copper doped titanium dioxide for enhancing the photovoltaic behaviour in solar cell, *Mater. Today Proce.*, 35, 66–68(2019). https://doi.org/10.1016/j.matpr.2019.06.377

Rajaram, P., Jeice, A. R. and Jayakumar, K., Influences of calcination temperature on titanium dioxide nanoparticles synthesized using Averrhoa carambola leaf extract: in vitro antimicrobial activity and UV-light catalyzed degradation of textile wastewater, *Biomass Convers. Biorefine.*, 14(17), 20665–20678(2023). https://doi.org/10.1007/s13399-023-04212-x

Rani, S. S., Vedavijaya, T., P, K. S., Shanmugasundaram, J., Deepalatha, C., Raju, M. G. and Sayana, S. B., A comprehensive analysis of phytochemical composition, acute toxicity assessment, and antioxidant potential of ethanolic extract of carica *Papaya* seeds, *Cureus*, 15(11), e49686(2023). https://doi.org/10.7759/cureus.49686

Saini, R. K., Sivanesan, I. and Keum, Y., Phytochemicals of Moringa oleifera: a review of their nutritional, therapeutic and industrial significance, *3 Biotech*, 6(2), 203(2016). https://doi.org/10.1007/s13205-016-0526-3

Singh, R. G., Negi, P. S. and Radha, C., Phenolic composition, antioxidant and antimicrobial activities of free and bound phenolic extracts of Moringa oleifera seed flour, *J. Func. Foods*, 5(4), 1883–1891(2013). https://doi.org/10.1016/j.jff.2013.09.009

Singhal, A., Kumari, A., Fahmi, N., Meena, P. and Meena, R., Synthesis of Nanomaterials: Green methods & amp; Technology, *Zenodo,* (2022). https://doi.org/10.5281/zenodo.5831859

Sławińska, N. and Olas, B., Selected Seeds as Sources of Bioactive Compounds with Diverse Biological Activities, *Nutri.*, 15(1), 187(2022). https://doi.org/10.3390/nu15010187

Srivastava, A. A., Bondarev, V. P., Kostyleva, E. I., Novikov, A. N., Fukina, D. G., Markov, A. N., Markin, Z. A. and Kazarina, O. V., Doped TiO_2 and oligoalkylhydrosiloxane-based surface modifiers with self-cleaning and hydrophobic properties, *Next Mater.*, 10, 101414(2025). https://doi.org/10.1016/j.nxmate.2025.101414

Tien, D. L. Q. and Le, T. N. B., Functional Cu-TiO_2 thin film coatings on glazed ceramic surfaces for visible-light photocatalytic and antibacterial applications, *Nano Exp.,* 7(1), 015010(2026). https://doi.org/10.1088/2632-959x/ae39f6

Wojcieszak, D., Mazur, M., Kaczmarek, D., Poniedziałek, A. and Osękowska, M., An impact of the copper additive on photocatalytic and bactericidal properties of TiO_2 thin films, *Mater. Sci. Poland*, 35(2), 421–426(2017). https://doi.org/10.1515/msp-2017-0041

Yoshida, K., Role of nanoparticle size in the photocatalytic degradation of pollutants, *J. Chem.*, 3(2), 12–20(2024). https://doi.org/10.47672/jchem.2405